Comment on "Nonlinear response of the polar ionosphere to large values of the interplanetary electric field" by C. T. Russell et al.

M. W. Liemohn and A. J. Ridley

Space Physics Research Laboratory, University of Michigan, Ann Arbor, Michigan, USA

Received 12 April 2002; revised 16 July 2002; accepted 25 September 2002; published 21 December 2002.

INDEX TERMS: 2463 Ionosphere: Plasma convection; 2760 Magnetospheric Physics: Plasma convection; 2784 Magnetospheric Physics: Solar wind/magnetosphere interactions; 2788 Magnetospheric Physics: Storms and substorms; *KEYWORDS:* Magnetosphere-ionosphere coupling, ionospheric electrodynamics cross polar cap potential saturation

Citation: Liemohn, M. W., and A. J. Ridley, Comment on ''Nonlinear response of the polar ionosphere to large values of the interplanetary electric field'' by C. T. Russell et al., *J. Geophys. Res.*, *107*(A12), 1460, doi:10.1029/2002JA009440, 2002.

1. Introduction

[1] The topic of the proper functional form of the ionospheric-magnetospheric response to solar wind conditions is a subject of much discussion and debate. While numerous studies over the decades have shown linear relationships [e.g., *Burton et al.*, 1975; *Reiff et al.*, 1981; *Boyle et al.*, 1997], others have found nonlinear relationships [e.g., *Hill et al.*, 1976; *Wygant et al.*, 1983; *Weimer*, 2001]. Recently, *Russell et al.* [2001] (hereinafter RLL) discuss a saturation effect in two high-latitude ionospheric parameters, the cross polar cap potential (CPCP) and the integrated Joule heating (IJH), for large values of the y-component of the interplanetary electric field (IEF), or the southward component of the interplanetary magnetic field (IMF B_z). They illustrate this effect by analyzing data and modeling results from five storms between 1995 and 1998, as well as evidence of saturation in other data sets. They conclude that the ionospheric response is saturated for IEF levels greater than 3 mV m^{-1}. Finally, they discuss the inner magnetosphere exhibiting a linear relationship with the IEF.

[2] With this comment, we hope to continue the discussion regarding the functional form of the magnetospheric response to the solar wind. We feel this is a critical issue of space physics, and it should be a top priority of our field to understand this relationship. That the CPCP exhibits nonlinearity and even saturates for large IEF values is not being disputed [see, e.g., *Liemohn et al.*, 2002]. However, the IEF at which the CPCP begins to saturate may be interpreted differently than presented by RLL. The nonlinear response may only be just beginning at 3 mV m^{-1}, where RLL state that it is in full effect. Additionally, there are several uses of data and model results discussed by RLL, which deserve further explanation. It is the hope of this comment to elucidate this analysis and to show that the data presented by RLL support the conclusion that nonlinear saturation effects become significant at substantially higher IEF values than 3 mV m^{-1}.

[3] Throughout this comment, the terms saturation and nonlinearity are taken to have distinct meanings. Saturation is when the slope of a curve asymptotically reaches zero. This is in contrast to the broader terms of nonlinearity and "the beginning of saturation," which refer to the deviation of the functional form away from a straight line.

0148-0227/02/2002JA009440

2. Discussion of the RLL Study

2.1. Curve Fit Comparison

[4] In Figures 2, 4, 6, 8, and 10 of RLL, hourly averages of CPCP and IJH are plotted against the corresponding IEF values (a plot for each storm interval included in the study). In this comment and in RLL, IEF is defined as the y-component of the cross product between solar wind velocity and the IMF. A double-layer curve is drawn through the data, with a low-level baseline (with zero or very little slope) for IEF < 0 followed by a sharp rise for small, positive IEF values, eventually flattening into a plateau (with little or no slope) at or near some saturation value at "high" IEF.

[5] The kink near IEF = 0 is quite reasonable, because the ionosphere and magnetosphere are known to have distinctly different responses to northward and southward IMF, corresponding to negative and positive IEF, respectively. Therefore, it is expected that the response of CPCP and IJH across the IEF = 0 level be dramatically different, and that the values below IEF = 0 should not be considered [see, e.g., *Friis-Christiansen et al.*, 1985; *Papitashvili et al.*, 1994; *Ridley et al.*, 2000].

[6] Of concern is the fit through the IEF >0 data. These data are quite dispersed, often with a large spread (>40 kV and >200 GW) at any given IEF value. The saturation values found for the five storms vary from 85 kV to at least 167 kV in CPCP and from 235 GW to at least 1415 GW in IJH. The IEF value where saturation is reached in the fits is also quite disparate, ranging from 3 mV m^{-1} to somewhere above 25 mV m^{-1}.

[7] It is worthwhile to compare the RLL curve fits with a linear regression of the CPCP and IJH values. The data and curve fits were digitally reconstructed and are shown in Figure 1 (dots and dashed lines, respectively). Also shown in Figure 1 is a linear fit to the IEF > 0 data points (solid lines), and a vertical dotted line at IEF = 0 is drawn on each subplot for reference. The standard deviations of the data from the two fits (that is, the root mean square error of the

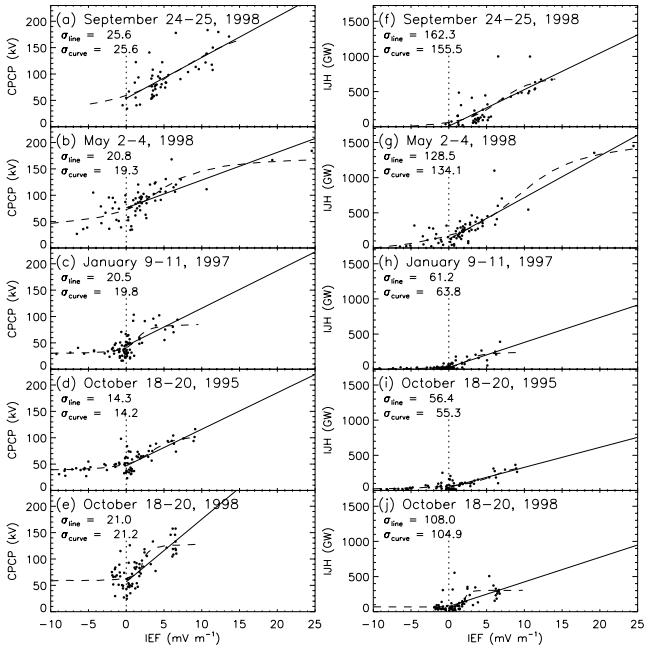

Figure 1. Data and curve fits for the five storms that RLL analyzed. The left-hand column shows CPCP values, and the right-hand column shows the IJH values. Data points are shown as black dots, with the RLL curve fits shown as dashed lines. Data with IEF >0 were used to produce a linear fit (solid lines). Standard deviations for each fit (solid and dashed) to the IEF >0 data are given in the upper corner of each plot. The dotted vertical lines are at IEF = 0, for reference.

fitted values minus the observed values, summed over the observed values with IEF > 0) are provided in each subplot. The linear fit has an equal or lower error for 4 of the 10 data sets, and in all but one of the 10 cases, the line and curve errors are within 5% of each other (for the CPCP of May 1998, they were within 10%). It is interesting to note that most of the linear fits are quite consistent with each other (except for the October storm), while the RLL fits are quite diverse. While each of these functional forms appears to fit some of these data sets better than others, neither functional form exhibits a clear superiority. From this, it appears that the chosen storm intervals are inconclusive in determining the linearity of the IEF dependence for these quantities.

[8] It is therefore concluded that the RLL fits do not support the claim of potential saturation at 3 mV m^{-1}. Only 2 of the RLL fits to CPCP saturate below 5 mV m^{-1}: January 1997 and October 1998. These events have no large IEF values, and the scatter is so large that it is difficult to clearly determine the onset of this saturation. The 2 events which have larger than 10 mV m^{-1} IEF values (September 1998 and May 1998) show that the CPCP has a linear dependence on the IEF up to at least 10 mV m^{-1}.

2.2. DE 2 Potential Drop

[9] Additional evidence of the CPCP saturating at a low IEF described in RLL comes from their interpretation of DE 2 data from *Weimer* [1995] and *Burke et al.* [1999]. Figure 12 of RLL shows a clear kink in the CPCP response to the IEF, with a steep slope from 0 to 3 mV m^{-1} and a much flatter curve beyond this value. This plot comes from equation (3) of *Burke et al.* [1999], which fitted data as a function of IMF clock angle (θ) for 4 specific IMF intensity bins. In each of these 4 fits, an offset (Φ_0) is calculated along with a "slope" versus $\sin^2(\theta/2)$. What was shown by RLL was this fitted CPCP for due southward IMF without the offset value Φ_0, plotted against IEF using the average solar wind velocities as calculated by *Burke et al.* [1999]. The offsets, however, vary between 22 and 32 kV, depending on the total IMF intensity. Because of this variation, this term should not be omitted from the analysis.

[10] Figure 2 shows the CPCP values as a function of IEF (for due southward IMF, using the average velocities) from the *Burke et al.* [1999] study, including the IMF strength-dependent Φ_0 (open diamonds). Also shown in Figure 2 are the *Burke et al.* [1999] fits to CPCP (again for due southward IMF) using a constant Φ_0 value as shown by RLL (RLL use $\Phi_0 = 0$, while Figure 2 shows $\Phi_0 = 27.5$ kV, the average of the IMF-dependent values). While the inclusion of the IMF-dependent offsets reduces the kink near 3 mV m^{-1}, it does not completely remove it. Both of these data sets, therefore, reveal a nonlinear functional form between the CPCP and the IEF. To quantitatively analyze these trends, each of these sets of points is fit to an exponential curve (which represents an asymptoting CPCP). The functional form and the best-fit coefficients are listed in the figure. By including the IMF-dependent Φ_0 values, the rate of convergence (1/T) toward the saturation potential (A) is 2.25 times slower than when this dependence is ignored. In addition, A is significantly higher and more consistent with the September and May 1998 storms presented by RLL.

[11] It should be noted that Figure 2 presents fits of binned data. That is, an average B_z and solar wind velocity were used for each IMF bin regardless of the real values for each data point. It is unclear how the results would change by using the original 2879 data points from *Weimer* [1995].

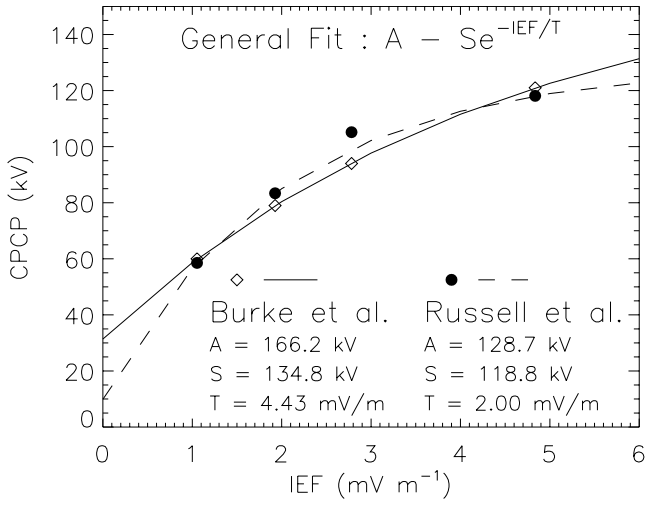

Figure 2. *Burke et al.* [1999] fits to CPCP data versus IEF for due southward IMF. The open diamonds are the CPCP values from the *Burke et al.* [1999] study. The black dots are the fitted values with a constant Φ_0 of 27.5 kV applied to each value (similar to that shown by RLL). Asymptotic exponential fits to each set of points are shown along with the coefficients.

In addition, ionospheric satellite measurements of the CPCP are always lower limits on the true CPCP during the pass (because the satellite track usually does not cross through the minimum and maximum potential locations), and it is unclear how a correction for this error would change this linearity analysis.

2.3. Combined View of the Five Storms

[12] By fitting the data sets for each storm individually, RLL are implicitly stating that the saturation level and rate of convergence toward it are storm-dependent. This is certainly true, as each storm has unique solar wind and IMF conditions, unique preexisting conditions, and a unique universal time and solar cycle phase placement. Many factors contribute to the development and magnitude of a magnetic storm, and so it is reasonable to consider each storm individually. However, it is also useful to combine the data from many storms in order to examine the general trend inherent in the ionosphere-magnetosphere response to solar wind disturbances.

[13] Figure 3 shows such a compilation. The CPCP values for IEF > 0 from all five storms examined by RLL are plotted here. As with Figure 1, the data are quite dispersed, with a range of about 100 kV at each IEF value below 7 mV m^{-1}, and a similar spread near 11 mV m^{-1}. Overlaid on these data are linear and exponential fits (solid and dotted lines, respectively). The best coefficients for these fits are

$$\mathrm{CPCP_{line}} = 58.1 + 7.29 \cdot \mathrm{IEF}$$

$$\mathrm{CPCP_{exp}} = 181.8 - 131.9\exp[-\mathrm{IEF}/10.11]$$

The standard deviations between the data and each of these lines are listed in the lower corner of the plot.

[14] It is seen that the exponential fit is best, although only marginally better than the linear fit. The difference between the exponential fit and the linear fit to the CPCP data from all five storms is rather small for IEF values below 10 mV m^{-1}. The two curves then diverge as the exponential fit flattens out, crossing quite close to the two data points above 15 mV m^{-1} (both from the May 1998 storm). Removing these two points from the linear fit reduces its standard deviation from the data to 23.5 (halving the disparity with the exponential curve's standard deviation). Figure 3 shows that the linear response function of the CPCP to the IEF is valid for IEF < 10 mV m^{-1}, while a saturated response is most appropriate above this threshold. This transition value of 10 mV m^{-1} is the approximate IEF in which the linear and exponential fits start to deviate from each other.

[15] For comparison, also shown in Figure 3 are the two exponential curve fits from Figure 2. The standard deviations for these curves are noticeably larger than the values for the other two curves, with the "Burke" curve (short dashed line) being marginally better than the "Russell" curve (long dashed line). The Burke curve fits the CPCP values at high IEF much better than the Russell curve, but it is too high at lower IEF. This lends support to the idea of a linear dependence at low IEF and an asymptotic dependence at high IEF, with the transition somewhere near an IEF of 10 mV m^{-1}, where the Burke curve saturates.

2.4. Inner Magnetosphere Linearity

[16] RLL state "The cold magnetospheric plasma in the plasmasphere and the hot plasma of the ring current seem strongly coupled to the IEF but the polar cap does not..." While there is very little discussion of this within the paper, we assume that this conclusion was made primarily on a rather good prediction of Dst for the September 1998 storm by the *Burton et al.* [1975] formulation, which has an energy input rate linearly proportional to IEF (shown in RLL Figure 1). This is a very reasonable conclusion from the results presented by RLL. Indeed, linear relationships have been found for the ring current energy input rate for IEF values up to ~10 mV m^{-1} [see, for instance, Figure 3 of *O'Brien and McPherron*, 2000]. This is because the large-scale convection in the magnetosphere, which moves the plasma sheet in close to the Earth to form the stormtime ring current, is driven by the dayside magnetic merging rate, which in turn is controlled by the IMF direction and magnitude (among other things). A linear inner magnetospheric dependence on IEF, therefore, is not surprising, and on average is the correct functional form up to 10 mV m^{-1} (e.g., the range of validity of the *O'Brien and McPherron* [2000] injection rate).

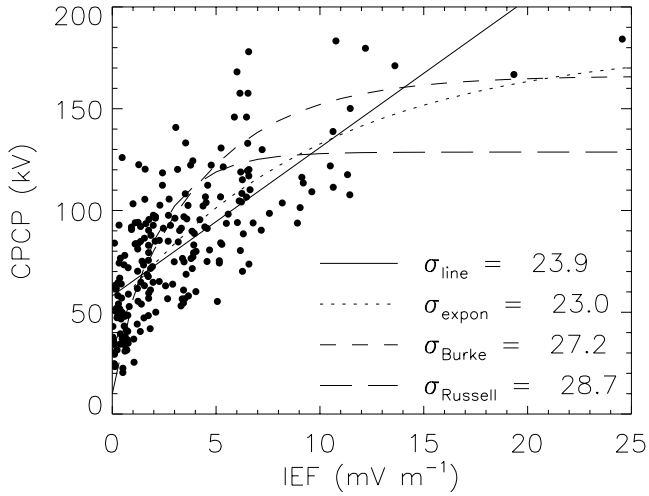

Figure 3. CPCP data from all five storms for IEF > 0. Linear and exponential curve fits to these data are also shown (solid dotted lines, respectively), along with the standard deviations from these lines. In addition, the "Burke" and "Russell" exponential fits from Figure 2 are overlaid (short and long dashed lines, respectively), along with the standard deviations between these lines and the data.

[17] Along with the convection strength, the other primary driving term of the stormtime ring current is the near-Earth plasma sheet density. Without particles to push in toward the Earth, Dst will not respond linearly to the CPCP or the IEF. Figure 4 shows the predicted (solid line) and observed (dotted line) Dst values for a larger interval around the September 1998 storm. The interval shown by RLL is bracketed by the two vertical dashed lines. It is clear that the *Burton et al.* [1975] algorithm did very well at predicting the initial growth of the storm. However, it completely mispredicted the recovery of the storm. During the second interval of large IEF, the plasma sheet density plummeted [see, e.g., Figure 3 of *Liemohn et al.*, 2001], and instead of increasing the ring current, the strong convection late in the storm rapidly evacuated the inner magnetosphere. A linear relationship cannot account for this type of interaction.

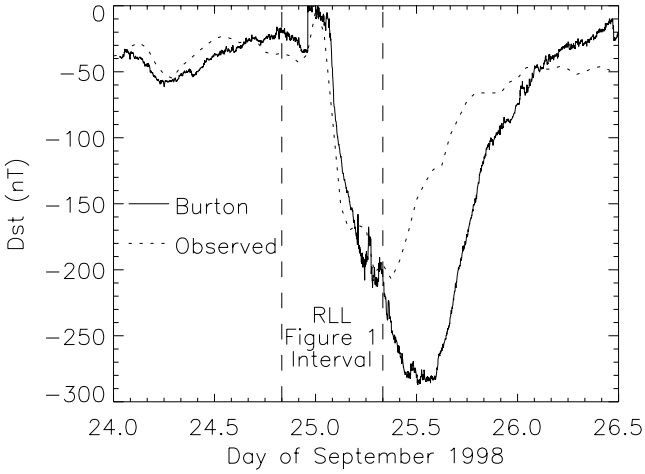

Figure 4. Dst for the 24–25 September 1998 storm. The dotted line is the observed value, and the solid line is the prediction using the algorithm of *Burton et al.* [1975]. The interval shown in Figure 1 of RLL is bracketed by the two vertical dashed lines.

While the ring current strength usually correlates well with the CPCP (and thus to the IEF), there are other factors influencing the ring current strength.

[18] In addition, if Figure 2 of *Burton et al.* [1975] (reprinted as Figure 2 of the accompanying reply) is examined closely, the 3 data points above an IEF of 8 mV m^{-1} could be showing signs of nonlinearity. The slope of these three points is significantly less that the slope of those below 8 mV m^{-1}. As in the case of Figure 1, these points may be fitted with either a line or an exponential, with approximately the same standard deviation.

3. Conclusion

[19] The efforts of Russell and coauthors to assess the response function of two ionospheric parameters to large values of the IEF are appreciated and applauded. This relationship is of critical importance for the study of the ionosphere and magnetosphere, and accurate space weather predictions cannot be made without a precise definition of this functional form. The RLL study adds to the body of knowledge on this topic and progresses the scientific community toward a consensus. While nonlinear saturation is most likely a real effect, saturation of the CPCP and the IJH at an IEF value of 3 mV m^{-1} is not supported by their selected data. It was shown above that a nonlinear response is only weakly evident in the CPCP results, and only for IEF > 10 mV m^{-1} (based primarily on 2 data points). Furthermore, a different usage of the data from the *Burke et al.* [1999] study indicates that the saturation in the CPCP, as observed by DE 2, occurs at IEFs of 10 mV m^{-1} of more. Also, Figure 3 of *Burke et al.* [1999] shows a rather good linear CPCP relationship against the *Kan and Lee* [1979] solar wind electric field throughout their plot range (up to 9 mV m^{-1}).

[20] Additionally, the discussion of the inner magnetosphere reacting linearly to the IEF, while the high latitude ionosphere does not, is not adequately supported. The chosen storm of September 1998 has an interval of very good linear Dst decrease with IEF, followed by an interval of very poor correlation. While a linear relationship is correct for an IEF < 10 mV m^{-1} on average, the September 1998 storm clearly shows that Dst decrease is not simply linearly related to the IEF. Other factors that do not scale linearly with IEF (for example, the near-Earth plasma sheet density) confound this relationship.

[21] **Acknowledgments.** This work was supported by National Science Foundation grants number ATM-0090165 and ATM-0077555 and by National Aeronautics and Space Administration grants NAG5-10297 and NAG-10850.

[22] Lou-Chuang Lee and Chin S. Lin thank William J. Burke for his assistance in evaluating this paper.

References

Boyle, C. B., P. H. Reiff, and M. R. Hairston, Empirical polar cap potentials, *J. Geophys. Res.*, *102*, 111, 1997.

Burke, W. J., D. R. Weimer, and N. C. Maynard, Geoeffective interplanetary scale sizes derived from regression analysis of polar cap potentials, *J. Geophys. Res.*, *104*, 9989, 1999.

Burton, R. K., R. L. McPherron, and C. T. Russell, An empirical relationship between interplanetary conditions and Dst, *J. Geophys. Res.*, *80*, 4204, 1975.

Friis-Christiansen, E., Y. Kamide, A. D. Richmond, and S. Matsushita, Interplanetary magnetic field control of high-latitude electric fields and currents determined from Greenland magnetometer chain, *J. Geophys. Res.*, *90*, 1325, 1985.

Hill, T. W., A. J. Dessler, and R. A. Wolf, Mercury and Mars: The role of ionospheric conductivity in the acceleration of magnetospheric particles, *Geophys. Res. Lett.*, *3*, 429, 1976.

Kan, J. R., and L. C. Lee, Energy coupling functions and solar-wind magnetosphere dynamo, *Geophys. Res. Lett*, *6*, 577, 1979.

Liemohn, M. W., J. U. Kozyra, M. F. Thomsen, J. L. Roeder, G. Lu, J. E. Borovsky, and T. E. Cayton, Dominant role of the asymmetric ring current in producing the stormtime Dst*, *J. Geophys. Res.*, *106*, 10,883, 2001.

Liemohn, M. W., J. U. Kozyra, M. R. Hairston, D. M. Weimer, G. Lu, A. J. Ridley, T. H. Zurbuchen, and R. M. Skoug, Consequences of a saturated convection electric field on the ring current, *Geophys. Res. Lett.*, *1348*, doi:10.1029/2001GL014270, 2002.

O'Brien, T. P., and R. L. McPherron, An empirical phase-space analysis of ring current dynamics: Solar wind control of injection and decay, *J. Geophys. Res.*, *105*, 7707, 2000.

Papitashvili, V. O., B. A. Belov, D. S. Faermark, Y. I. Feldstein, S. A. Golyshev, L. I. Gromova, and A. E. Levitin, Electric potential patterns in the northern and southern polar regions parameterized by the interplanetary magnetic field, *J. Geophys. Res.*, *99*, 13,251, 1994.

Reiff, P. H., R. W. Spiro, and T. W. Hill, Dependence of polar cap potential drop of interplanetary parameters, *J. Geophys. Res.*, *86*, 7639, 1981.

Ridley, A. J., G. Crowley, and C. Freitas, A statistical model of the ionospheric electric potential, *Geophys. Res. Lett.*, *27*, 3675, 2000.

Russell, C. T., J. G. Luhmann, and G. Lu, Nonlinear response of the polar ionosphere to large values of the interplanetary electric field, *J. Geophys. Res.*, *106*, 18,495, 2001.

Weimer, D. R., Models of high-latitude electric potentials derived with a least error fit of spherical coefficients, *J. Geophys. Res.*, *100*, 19,595, 1995.

Weimer, D. R., An improved model of ionospheric electric potentials including substorm perturbations and application to the Geospace Environment Modeling November 24, 1996, event, *J. Geophys. Res.*, *106*, 407, 2001.

Wygant, J. R., R. B. Torbert, and F. S. Mozer, Comparison of S3-3 polar cap potential drops with the interplanetary magnetic field and models of magnetopause reconnection, *J. Geophys. Res.*, *88*, 5727, 1983.

M. W. Liemohn and A. J. Ridley, Space Physics Research Laboratory, University of Michigan, 2455 Hayward Street, Ann Arbor, Michigan, USA. (liemohn@umich.edu; ridley@umich.edu)